Modelling DCE-MRI Arterial Input Functions in Rats

D. McGrath[1], T. Lacey[2], D. Bradley[2], C. Taylor[1], G. Parker[1]

[1]Imaging Sciences and Biomedical Engineering, University of Manchester, Manchester, Lancashire, United Kingdom, [2]Astrazeneca, Alderley Park, Macclesfield, Cheshire, United Kingdom

INTRODUCTION

DCE-MRI is routinely used in phase I/II studies of anti-vascular therapies in cancer due to its ability to quantify parameters associated with vascular function non-invasively [1]. When compartmental modelling is employed it is necessary to identify an appropriate arterial input function (AIF), a non-trivial process whose success may impact on the accuracy and power of any study. In this work we assess the effects of using various forms of AIF model compared with using experimentally acquired high temporal resolution AIF data and make recommendations based on these observations.

METHODS

DCE-MRI semi keyhole data acquired using Magnevist (Gadopentetate Dimeglumine, Schering), acquired from a colorectal LoVo human tumour xenograft rat model using a 4.7 T Varian system at AstraZeneca UK was chosen to evaluate a range of AIF modelling approaches. Using 8 animals, in accordance with Home Office (Scientific Procedures, UK) Act 1986, 2 repeat sets of saturation recovery DCE-MRI data 24 hours apart, were acquired for 5 min (TR/TE 13.9/2.3ms, α 15°, sagittal, saturation angle 90°, sagittal SlThk 10mm, delay time 10ms, field-of-view 6cm^2, slice thickness 5mm**,** 2 averages, 128x96 read and phase encoding steps, respectively (zero filled to 128x128) [7,8], temporal resolution of 0.5s/image), during which time Magnevist was administered to the tail vein. Concentration calibration tubes present during the acquisition were used to convert the tumour signal and AIF into Gd concentration. Four different AIF models were used to fit the data and compared with the use of the raw AIF data by calculating the parameters from the extended Kety model [2] i.e. v_p (fractional blood plasma volume), k^{trans} (volume transfer constant) and v_e (fractional extravascular, extracellular space volume). The AIF models used were (1) bi-exponential [3], (2) two segments of linear fit followed by bi-exponential (Su model) [4], (3) a single Gaussian plus exponential modulated by sigmoid, (4) sum of two Gaussians plus an exponential modulated by sigmoid [5]. Models 3 and 4 are described by the following equation with $N = 1$, and 2 respectively: $C_b(t) = \sum_{n=1}^{N} \frac{A_n}{\sigma_n\sqrt{2\pi}} \exp\left(\frac{-(t-T_n)^2}{2\sigma_n^2}\right) + \frac{\alpha \exp(-\beta t)}{(1+\exp(-s(t-\tau)))}$ The second Gaussian in model 4 is designed to model a reflow peak, if present. The AIF models were fitted and the extended Kety model solution found using a Levenberg-Marquardt algorithm. The first experiments aimed to establish the competence of each model in approximating the acquired AIF. The kinetic parameters (k^{trans}, v_e and v_p) were derived using the acquired AIF data and compared with those estimated using each AIF model (fitted to the individuals data). In the second experiment a population average AIF was computed, to which each of the models were fitted. Together with the mean acquired AIF, each model was then used to derive kinetic parameters for every individual and the parameters again compared with those derived using the actual acquired AIF. Finally the individual AIF and population results were analyzed for repeatability by calculating the within subject co-efficient of variation (wCV) between the repeat scans, for each kinetic parameter [6]. The *wCV* values were calculated using the formula, [6], $wCV = \text{antilog}(dsd/\sqrt{2}) - 1$, where *dsd* is the mean squared difference (of logs) of the parameter values. The between subject variance is also presented for each model (bVar),as a surrogate sensitivity measure.

RESULTS

Figure 1 shows example AIF model fits. Figure 2 illustrates the mean parameter differences between the model and acquired AIF as a percentage of the acquired AIF value together with 95% confidence intervals. Figure 3 summarises the population average AIF experiment results and table 1 provides the results of the intra-subject, inter-subject experiment. In both table sections the lowest wCV and highest bVar obtained are printed in bold.

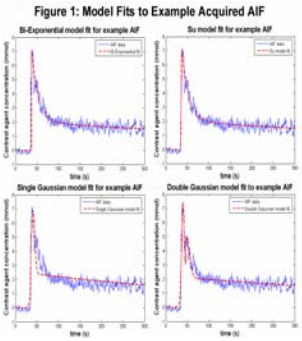

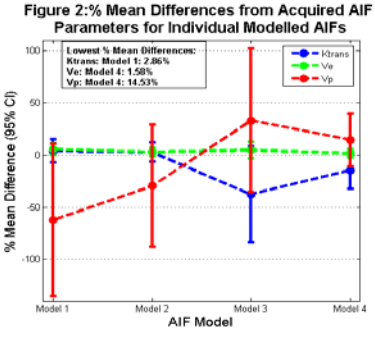

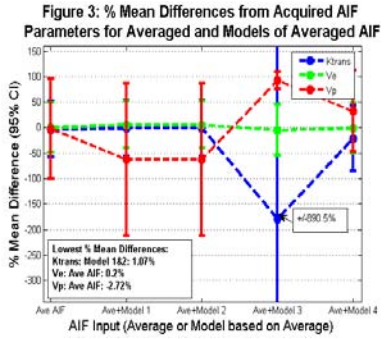

DISCUSSION AND CONCLUSION

The results from the first experiment (figure 2) indicate that, for k^{trans} and v_e, the bi-exponential models provide closest agreement to the parameters derived using the measured AIF (v_p is poorly measured with this contrast agent). The results further indicate that the Gaussian models are likely to provide biased, over estimates of k^{trans}. The results from the population experiments (figure 3) also suggest a preference for the bi-exponential models (which perform identically) over the Gaussian models. A possible explanation for the poorer performance of the double Gaussian model is that the second peak is designed to model recirculation effects which are unseen in our data. Table 1 further supports the arguments for bi-exponential modelling. Overall the best repeatability values are obtained with the bi-exponential models applied to the population average. By including the between subject variance we are attempting to verify that lower within subject variation is not caused by removal of critical features from the AIF. Generally these models reduce the within subject (between the 2 scans) variance whilst increasing or at least maintaining the between subject variance. It is important to note the high level of variability present when using either an averaged AIF or model fitted to the averaged AIF data, compared with that achieved using the acquired AIF. Despite the low overall bias between the approaches, this level of variability suggests even within a well designed control group there can be significant variability which may impact on the power of a study. Future work will include comparison of the variability in parameters after drug treatment with that obtained using different AIF models.

Table 1:

		v_p		k^{trans}		v_p	
	Model Type	**wCV**	**bVar**	**wCV**	**bVar**	**wCV**	**bVar**
Individual AIF Model	Raw Data	0.6651	3.7711e-004	0.6239	4.2129e-006	**0.1984**	**0.0107**
	(1)	**0.4849**	**8.1102e-004**	0.6269	4.0886e-006	0.1989	0.0092
	(2)	0.5763	5.5909e-004	0.6232	4.0984e-006	0.2088	0.0100
	(3)	5.6486	1.3665e-004	0.6652	**1.0906e-005**	0.2100	0.0104
	(4)	0.7616	2.3150e-004	**0.5718**	6.3836e-006	0.2014	0.0106
Population Average AIF Model	Ave Raw Data	0.5851	7.0478e-004	0.2716	5.0122e-006	0.1437	0.0013
	(1)	**0.4097**	**0.0013**	**0.2603**	4.3239e-006	**0.1347**	0.0136
	(2)	**0.4097**	**0.0013**	**0.2603**	4.3239e-006	**0.1347**	0.0136
	(3)	1.7950	2.5584e-005	1.8786	**2.7633e-004**	0.1648	**0.0176**
	(4)	0.8082	4.3622e-004	0.2783	7.4460e-006	0.1524	0.0162

REFERENCES

1.Jackson A et al, *Dynamic contrast-enhanced magnetic resonance imaging in oncology* (Springer, Berlin); 2005, **2.** Tofts PS et al, *J. Magn. Reson. Imaging,* 10, 223-232, 1999; **3.** Wedeking P et al, *Magn. Reson. Imaging*.,8, 567-75, 1990; **4.** Su M-Y et al, *Mag. Res. Med.* 32:714-724, 1994. **5.** Parker GJ et al, *Proc. ISMRM,* 2101; 2005. **6.** Galbraith S et al, *NMR Biomed.* 15:132-142, 2002;**7.** Kuribayashi H et al. *Magn. Reson. in Medical Sciences* 2004;3:207-210; **8.** Bradley et al., *Proc. ISMRM*, 546, 2004.